elements as a capacitor, but resonances indicate that the PCB via model needs to be modified at frequencies above 2 GHz.

IV. Conclusion

The determination of the characteristic impedance of the TRL standards is important since it directly affects the accuracy of the de-embedded results. The enhancement of TRL presented here incorporates the frequency dependence of the characteristic impedance and includes transmission line loss.

References

[1] G. F. Engen and C. A. Hoer, "Thru-reflect-line: An improved technique for calibrating the dual six-port automatic network analyzer," *IEEE Trans. Microwave Theory Tech.*, vol. MTT-27, pp. 987–993, Dec. 1979.

[2] W. J. Getsinger, "Measurement and modeling of the apparent characteristic impedance of microstrip," *IEEE Trans. Microwave Theory Tech.*, vol. MTT-31, pp. 624–632, Aug. 1983.

[3] I. Bahl and S. Stuchly, "Analysis of a microstrip covered with a lossy dielectric," *IEEE Trans. Microwave Theory Tech.*, vol. MTT-28, pp. 104–109, Feb. 1980.

[4] B. Bianco, L. Panini, M. Parodi, and S. Ridella, "Some considerations about the frequency dependence of the characteristic impedance of uniform microstrips," *IEEE Trans. Microwave Theory Tech.*, vol. MTT-26, pp. 182–185, Mar. 1978.

[5] J. P. Mondal and T-H. Chen, "Propagation constant determination in microwave fixture de-embedding procedure," *IEEE Trans. Microwave Theory Tech.*, vol. 36, pp. 706–714, Apr. 1988.

[6] T. Wang, R. F. Harrington, and J. R. Mautz, "Quasi-static analysis of a microstrip via through a hole in a ground plane," *IEEE Trans. Microwave Theory Tech.*, vol. 36, pp. 1008–1013, June 1988.

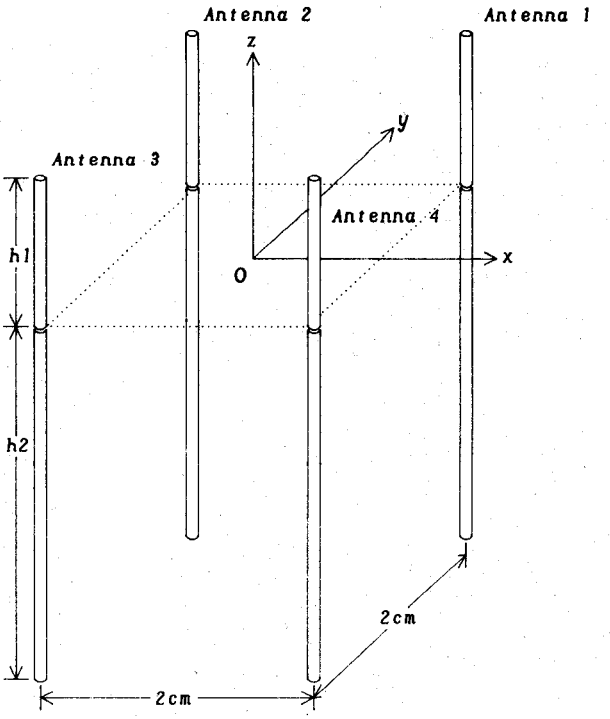

Fig. 1. Square array of four interstitial antennas. The radiating gaps of the antennas are in the lateral plane $z = 0$, and the definition of the coordinates is shown. Details of each antenna are discussed in the text.

Microwave Hyperthermia Induced by a Phased Interstitial Antenna Array

YANG ZHANG, WILLIAM T. JOINES, MEMBER, IEEE, AND JAMES R. OLESON

Abstract—**An interstitial microwave antenna array for hyperthermia cancer treatment is investigated. The purpose is to generate both uniform and controlled nonuniform temperature distributions in biological tissue by modulating the phases of the signals applied to each antenna. The array has four antennas positioned on the corners of a 2 cm square. The distributions of absorbed power within the arrays are computed and then converted into temperature distributions through a heat conduction simulation. The temperature patterns over phantom muscle are presented in both the lateral plane (perpendicular to the antennas) and the axial plane (parallel to the antennas). It has been found that, by proper phase modulation of RF signals applied to each antenna, a uniform heating can be produced in the entire array volume. Also, a peripheral heating pattern may be generated around the array, again by using the proper phase modulation.**

I. Introduction

Microwave-induced hyperthermia has received increased attention in recent years in the treatment of cancer. The primary objective for any hyperthermia treatment is to raise the tumor temperature above 42–43°C for an extended period while keeping the temperature in the surrounding normal tissue well below 43°C. These temperatures can be directly cytotoxic and can potentiate the effect of radiation therapy [1], [2].

A commonly used heating method is interstitial or invasive hyperthermia, where thin coaxial dipole antennas, operating at microwave frequencies (300–2450 MHz), are inserted into the tissue [3]. The antennas are made from coaxial cables that are about 1 mm in diameter and have a radiation gap or gaps in the outer conductor. The antennas are inserted into the tumor through brachytherapy catheters that are nylon tubes about 2 mm in outer diameter used for implantation of iridium for radiation therapy. Through the application of interstitial antennas, various interesting heating patterns may be obtained by using the constructive and/or destructive interference features of the EM fields radiated from the antennas [4], [5]. By changing the driving phase of the signal applied to each antenna, the phase-coherent spot (where constructive interference occurs) may be shifted well away from the center of a 2 cm square array. By varying the relative phase between each antenna, sequentially in time, a more uniform heating pattern may be generated, as well as certain nonuniform heating patterns that may be required for specific applications [6], [7]. In this paper, we investigate the techniques for generating uniform and nonuniform (such as the type in [6] and [7]) heating patterns for a four-antenna array, as shown is Fig. 1. Four interstitial antennas are positioned on the corners of a 2 cm square. The antennas operate at 915 MHz. Theoretical calculations of *SAR* and thermal conduction are performed using properties of phantom muscle tissue. Therefore, the predicted temperature distributions do not represent what they would be in perfused tissue; rather they show what can be accomplished with the phased interstitial antenna arrays when blood flow is neglected.

Manuscript received May 30, 1989; revised September 14, 1989. This work was supported by PHS Grant 1 pol CA 42745-01A1, awarded by the National Cancer Institute, DHHS.

Y. Zhang and W. T. Joines are with the Department of Electrical Engineering, Duke University, Durham, NC 27706.

J. R. Oleson is with the Division of Radiation Oncology, Department of Radiology, Duke University Medical Center, Durham, NC 27710.

IEEE Log Number 8932010.

0018-9480/90/0200-0217$01.00 ©1990 IEEE

II. Methods

A number of researchers have worked toward characterizing the interstitial antenna [4], [5], [8], [9] and two models are currently used to simulate the radiation pattern. With one of the models, the interstitial applicator is simulated as a symmetric dipole; i.e., the antenna is represented as two arms of equal length, the same as the gap-to-tip length of the antenna [5], [8]. Although this model yields agreement between theory and experiment in lateral planes near the antenna tip [5], no comparison along the axis of the antenna has been reported. The second model currently used represents the interstitial antenna as an asymmetric dipole; i.e., the antenna is simulated as having two arms of unequal length, one being the gap-to-tip length and the other, somewhat longer arm being determined by experiment [9], [4]. Intuitively, this approach is quite reasonable because the physical structure of the interstial antenna is asymmetric about the radiation gap along the antenna axis. As reported in [4] and [9], power deposition calculations based upon the asymmetric model, for single antennas and for phased antenna arrays, yield close agreement with experiment in both the lateral plane (the plane perpendicular to the antennas) and the axial plane (the plane parallel to the antennas).

In this study, the asymmetric dipole model is again used to simulate each antenna in an array. Since the detailed derivations are presented in [9] and [4] for the single antenna and the four-antenna array, we shall not repeat the theory. Fig. 1 illustrates the associated coordinate system. The junctions of antennas 1–4 are located, respectively, at $(a, a, 0)$, $(-a, -a, 0)$, $(-a, -a, 0)$, and $(a, -a, 0)$, where a is half of the distance between two adjacent antennas. If the junction position of the antennas is represented as $(x_{0i}, y_{0i}, 0)$, where $i = 1, 2, \cdots, 4$, the total electric field components for the antenna array at point (x, y, z) may be expressed as

$$E_x = \sum_{i=1}^{4} \frac{x - x_{0i}}{R_i} E_{ri} e^{j\theta_i} \tag{1}$$

$$E_y = \sum_{i=1}^{4} \frac{y - y_{0i}}{R_i} E_{ri} e^{j\theta_i} \tag{2}$$

and

$$E_z = \sum_{i=1}^{4} E_{zi} e^{j\theta_i} \tag{3}$$

where θ_i are the time phase angles of the fields at each antenna. The incident electric field components in the r (radial) and z (axial) directions, E_{ri} and E_{zi}, respectively, are computed by [9, eqs. (2) and (3)] for each antenna, and

$$R_i = \sqrt{(x - x_{0i})^2 + (y - y_{0i})^2}\,. \tag{4}$$

The power absorbed per unit mass (SAR) is determined by

$$SAR = \frac{\sigma}{2\rho}\left(|E_x|^2 + |E_y|^2 + |E_z|^2\right) \tag{5}$$

where σ is the electrical conductivity of the biological tissue, and ρ is the density of the medium. Equation (5) yields the spatial SAR distribution within the array as a function of position relative to the antennas.

The temperature distribution is obtained by a heat conduction simulation. The electrical network analogy to heat flow within phantom muscle tissue reported in [4], [10], and [11] is used. With this technique, the thermal system is represented by an electric circuit mesh. The absorbed microwave power (or SAR times density times block volume), thermal resistance, heat capacitance, and temperature are simulated, respectively, as current source, electrical resistance, and potential. Therefore, solving the equivalent electric network yields the temperature distribution [4].

III. Results

The interstitial antennas used in our simulation have an outer diameter of 0.95 mm, with the gap-to-tip length $h_1 = 1.989$ cm, and $h_2 = 13.0$ cm. The determination of h_2 will not be presented here since it was discussed at length in [9]. The catheter has an inner diameter of 1.168 mm and an outer diameter of 1.61 mm. The catheter is made of polypropylene, with relative permittivity of 2.55 [12]. The ambient medium is muscle equivalent tissue of relative permittivity 51 at 915 MHz, conductivity 1.28 S/m, and density 970 kg/m^3.

The SAR calculation is performed over an area of 4 cm by 4 cm in the lateral plane, with a grid size of 2 mm by 2 mm. In the axial plane, the SAR values are computed over an area of 4 cm by 14 cm with a grid size of 2 mm by 4 mm. The SAR data are then used in the heat conduction simulation. The temperature calculations are done, in the lateral and axial planes respectively, at the same resolutions as for the SAR computation, but over a larger area. An area of 6 cm by 6 cm is simulated in the lateral plane, and 6 cm by 16 cm in the axial plane. The ambient temperature is enforced on the boundary. We have confirmed by experiment that enforcing the boundary conditions at such a distance does not affect the temperature calculations. For a typical temperature simulation in the axial plane, we used 1161 nodes, 2389 thermal resistors, 1160 thermal capacitors, and 756 heat-flux current source inputs (microwave energy absorbed in each block). Both the SAR and the temperature values are computed on a Data General computer (MV20000). The SAR calculation in one plane takes about 10 hours of CPU time, whereas a CPU time of 3 hours is required to compute each temperature distribution. The temperature patterns presented below are the normalized temperature increments with respect to their maximum values, and are plotted as percentage contour lines.

We used phase modulation to change the focal spots to generate various heating patterns, namely, the uniform and peripheral temperature distributions in the antenna array. Fig. 2 shows the theoretical patterns of uniform temperature distribution generated through three consecutive heatings:

1) driving the four antennas in phase for 50 percent of the heating time;
2) driving antennas 1 and 4 at 180° and antennas 2 and 3 at 0° for 25 percent of the heating time;
3) driving antennas 1 and 2 at 180° and antennas 3 and 4 at 0° for 25 percent of heating time.

This phase modulation procedure generates a rather uniform pattern in the array volume. Fig. 2(a) illustrates the result in the lateral plane and shows that the 90 percent isotherm encloses the entire array. Also, the temperature varies by less than 10 percent within the array. In the axial plane (Fig. 2(b)), the 85 percent isotherm line encloses an area of 2 cm by 2 cm. Therefore, a uniform temperature distribution may be obtained within a volume of 2 cm × 2 cm × 2 cm. The associated SAR distribution in the lateral plane $z = 0$ is shown in Fig. 3(a). For comparison, Fig. 3(b) is reproduced from [5, fig. 4(b)]. With this we can only

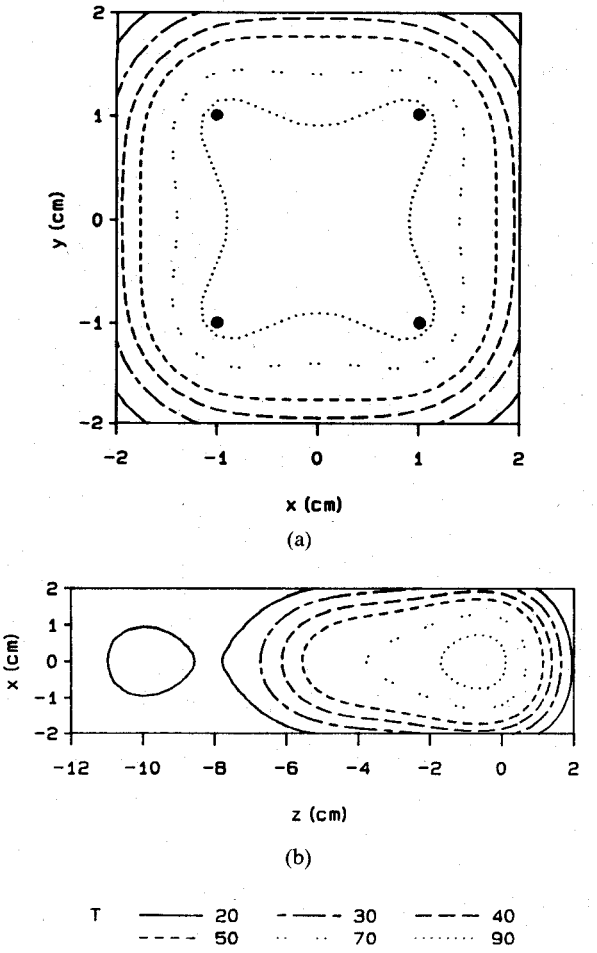

Fig. 2. Uniform temperature distribution generated from the four-antenna array with the phase modulation discussed in the text. The temperature increments are normalized to their maximum, and plotted in percentage contours. (a) In the lateral plane. (b) In the axial plane.

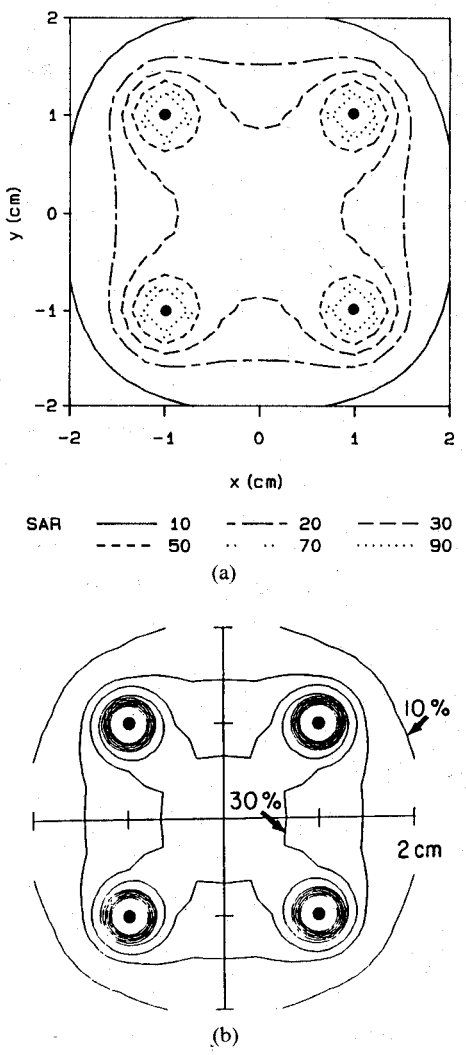

Fig. 3. Comparison of the *SAR* distribution in the lateral plane. (a) *SAR* pattern generated with the phase modulation that produces Fig. 2(a). (b) *SAR* pattern reproduced from [5] with different phase modulation.

compare our results in the lateral plane, since the other group's *SAR* information in the axial plane is not available.

In Fig. 4, a peripheral type of heating pattern, generated from the four-antenna array, is shown. The heating procedure used for generating the pattern is:

1) driving antennas 1 and 4 in phase at 180° and antennas 2 and 3 in phase at 0° for 50 percent of the heating time;
2) driving antennas 1 and 2 in phase at 180° and antennas 3 and 4 in phase at 0° for 50 percent of the heating time.

In the lateral plane (Fig. 4(a)), an elevated isotherm (above 70 percent of maximum) occurs along the boundary of the array, while a constant power deposition (between 60 and 70 percent) is observed at the array center. In the axial plane (Fig. 4(b)), elevated power (90 percent and above) is obtained in two areas along the edges of the array. This elevated peripheral heating extends about 2 cm along the antennas. An isotherm of more than 60 percent is achieved over a volume of 3 cm × 3 cm × 4 cm, with a maximum heating shell 0.5 cm thick over the boundary.

IV. Discussion

It has been reported previously [4] that the heating patterns of the four-antenna array, predicted by the theory upon which this paper is based, show excellent agreement with experiments for a number of phase modulations. Therefore, the results presented in this paper are derived theoretically only. For the four-antenna array operated at 915 MHz, the maximum *SAR* occurs at the center of the array, if the antennas are driven coherently in phase [4], [5]. This type of power deposition may not be optimal in that an elevated power deposition at the edges of a tumor where blood flow is high would lead to a more uniform temperature elevation.

As presented in this paper, uniform temperature distributions, and peripheral heating patterns with maximum power deposition around the boundary, may be generated by using various phase modulations. The results were obtained through simulations on phantom muscle tissue in which thermal conduction with no blood flow was considered. The actual temperature distributions in tumors will vary due to blood flow and inhomogeneity of the tissue. In Fig. 2, the uniform temperature distributions are shown. Three heating intervals with the phase modulation described in the previous section are necessary to generate the uniform temperature distribution in the array. The proposed phase modulation shifts the focal spot to the desired location. When the local maximum is rotated rapidly around the array volume, the time-averaged temperature distribution becomes uniform. In Fig. 2(a), the temperature changes by less than 10 percent within the entire array. Outside the array, the temperature decreases monotonically. From the heating patterns of Fig. 2(a) and (b), we may

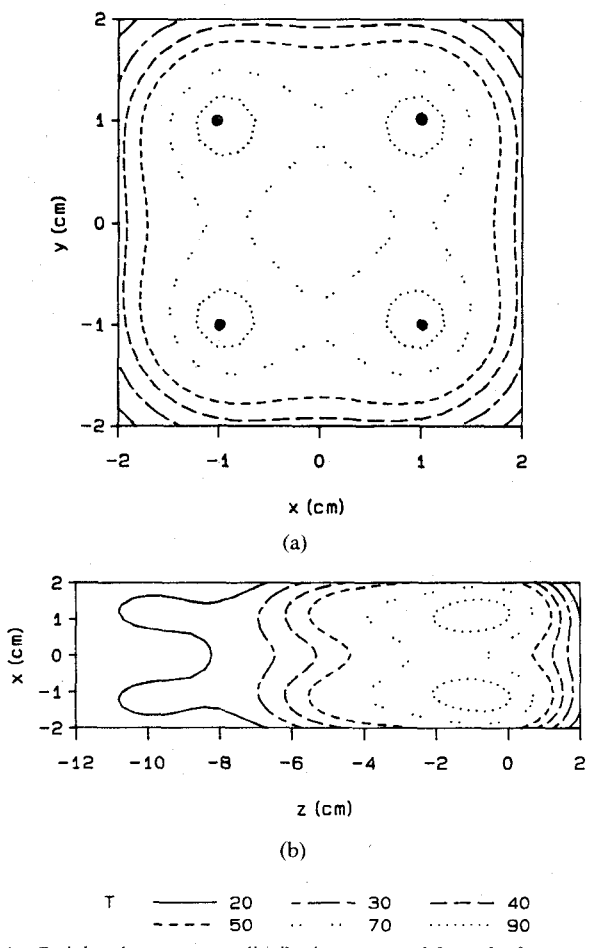

Fig. 4. Peripheral temperature distribution generated from the four-antenna array with the phase modulation discussed in the text. The temperature increments are normalized to their maximum, and plotted in percentage contours. (a) In the lateral plane. (b) In the axial plane.

conclude that the four-antenna array yields a uniform temperature distribution (less than 10 percent change in temperature) over a volume of 2 cm × 2 cm × 2 cm. Since the antenna gaps are in the plane $z = 0$, the volume of uniform temperature is located below the plane $z = 0$ (Fig. 1 and Fig. 2(b)). The temperature drops rapidly toward the tip of the antennas. It is not possible to attain a uniform temperature distribution in a volume near the tips of the antennas.

In Fig. 3, a comparison between the present result and that in [5] is made. Fig. 3(a) is the *SAR* distribution obtained by using the same phase modulation that produced the temperature pattern shown in Fig. 2(a). Fig. 3(b) is the *SAR* pattern reproduced from [5, fig. 4(b)]. With the *asymmetric* dipole model and the phase modulation described in this paper, more than 30 percent of the *SAR* is deposited over an area of 9 mm by 9 mm (Fig. 3(a)). With the *symmetric* dipole model and the phase modulation in [5], 30 percent of the *SAR* occurred over a smaller area of 6 mm by 6 mm (Fig. 3(b)). Therefore, the area that has a uniform *SAR* distribution has been expanded by more than 125 percent. A similar comparison cannot be made in the axial plane, because the *SAR* information in the axial plane is not available from [5]. The phase modulation technique with increased volume of uniform *SAR* should make the four-antenna array much more efficient in treating tumors. Although the local *SAR* maximum near each antenna cannot be eliminated through phase modulation, as shown is Fig. 3(a), thermal conduction will level these peaks, and the resulting temperature is quite uniform (Fig. 2(a)).

Ocheltree *et al.* have suggested, for simple geometries with spatially uniform blood flow and a uniform temperature elevation in tumor, that the *SAR* must have its maximum at the tumor edge and a small but constant value everywhere inside the tumor [6], [7]. The peripheral heating cannot be generated without phase modulation [4], [5]. With proper phase modulation applied to the antennas, however, it becomes possible to shift the focal spot around the antenna array. Fig. 4 shows that the maximum power deposition on the array margins is achieved. More than 70 percent of maximum temperature takes place around the periphery of the array, while almost constant temperature (between 60 and 70 percent) is observed in the central part of the array (Fig. 4(a)). This is almost the ideal heating pattern suggested in [6] and [7]. The marginal heating extends more than 4 cm (for the 70 percent contour line in Fig. 4(b)) in the axial direction. Therefore, the four-antenna array is suitable for small, ellipsoidal tumors. The antennas should be positioned around the edges of the tumor, and in parallel with the major axis of the tumor.

Although only temperature distributions in phantom muscle tissue are shown in this paper, it is known that the temperature distribution in phantom tissue represents that of real tissue with no blood flow, whereas the *SAR* distribution in phantom tissue illustrates the case of infinite blood flow. The uniformity of *SAR* distributions are also improved with the proposed phase modulations. The peripheral *SAR* distributions are obtained as well (not shown). With the *SAR* distributions and the temperatures distributions in phantom tissue, we have considered the two extreme cases (infinite blood flow and zero blood flow). The temperature distribution in perfused tissue would be represented by combinations of these two cases, and empirical adjustment of the phase modulation would be necessary in practice.

V. Conclusion

We have extended the theory of the insulated, asymmetric dipole antenna embedded in a dissipative dielectric medium to interstitial antenna arrays used for microwave-induced hyperthermia. The phase modulation technique is incorporated into the theory for the four-antenna square array. It is found that with proper phase modulation at 915 MHz, both uniform and peripheral temperature distributions can be generated. Compared with published data from other groups, an improved uniform *SAR* distribution over a larger area has been achieved with the phase modulation technique proposed in this paper. For the uniform heating pattern, the temperature changes by less than 10 percent in the entire array. For the peripheral heating pattern, a temperature of more than 70 percent of the maximum occurs around the boundary. Inside the elevated heating shell, the temperature is lower and quite uniform. The same phenomena are observed in the axial direction along the antennas. The heated volume (60 percent heating and above) extends a few centimeters in the axial direction. The phase modulation techniques required for producing the various temperature distributions depend upon both array types and the patterns to be generated. The results here demonstrate the potential of these techniques for producing *SAR* distributions that may be used to optimize temperature distribution in specific applications.

References

[1] G. M. Hahn, *Hyperthermia and Cancer*. New York: Plenum Press, 1982, pp. 1–285.

[2] C. T. Coughlin *et al.*, "Interstitial hyperthermia in combination with brachytherapy," *Radiology*, vol. 148, pp. 285–288, 1983.

[3] J. W. Strohbehn and J. A. Mechling, "Interstitial techniques for clinical hyperthermia," in *Handbook of Techniques for Clinical Hyperthermia*,

J. W Hand and J. R James, Eds. London: Research Studies Press, 1986, pp 210–279.

[4] Y. Zhang, W. T Joines, and J. R. Oleson, "Calculated and measured temperature distribution of a phased interstitial antenna array," *IEEE Trans. Microwave Theory Tech.*, vol. 38, pp 69–77, Jan. 1990.

[5] B. S Trembly, A. H. Wilson, J. M Havard, K. Sabatakakis, and J. W. Strohbehn, "Comparison of power deposition by in-phase 433 MHz and phase-modulated 915 MHz interstitial antenna array hyperthermia systems," *IEEE Trans. Microwave Theory Tech* , vol. 36, pp. 908–916, May 1988.

[6] K. B Ocheltree and L. A. Frizzell, "Determination of power deposition patterns for localized hyperthermia: A steady-state analysis," *Int. J. Hyperthermia*, vol. 3, no. 3, pp 269–279, 1987.

[7] K B. Ocheltree and L A Frizzell, "Determination of power deposition patterns for localized hyperthermia: A transient analysis," *Int. J. Hyperthermia*, vol. 4, no. 3, pp. 281–296, 1988

[8] R. W. P. King, B. S. Trembly, and J. W. Strohbehn, "The electromagnetic field of an insulated antenna in a conducting or dielectric medium," *IEEE Trans. Microwave Theory Tech.*, vol. MTT-31, pp. 574–583, July 1983.

[9] Y. Zhang, N. V. Dubal, R. Takemoto-Hambleton, and W T. Joines, "The determination of the electromagnetic field and *SAR* pattern of an interstitial applicator in a dissipative dielectric medium," *IEEE Trans. Microwave Theory Tech.*, vol. 36, pp. 1438–1444, Oct. 1988.

[10] R. J. Spiegel and M B. E. Fatmi, "A three-dimensional finite-difference thermoregulatory model of a squirrel monkey," *Int J. Radiation Oncology Biol. Phys.*, vol. 12, no. 6, pp. 983–992, June 1986.

[11] J. P. Holman, *Heat Transfer*, 3rd ed. New York: McGraw-Hill, 1972, ch. 4.

[12] *Reference Data for Radio Engineers*, Howard W. Sams & Co , Inc., Indianapolis, IN, 46268, 1975, pp 4–28.